Experimental Segregation Profiles in Bubbling Gas-Fluidized Beds

Gustavo G. Joseph, José Leboreiro, Christine M. Hrenya, and Andrea R. Stevens
Dept. of Chemical and Biological Engineering, University of Colorado at Boulder, Boulder, CO 80309

DOI 10.1002/aic.11282
Published online September 13, 2007 in Wiley InterScience (www.interscience.wiley.com).

Species segregation measurements were performed in a fluidized bed composed of a binary, Geldart B mixture. Three system types were explored: size segregation, density segregation, and combined size/density segregation (with the smaller species denser and lighter). Glass and polystyrene mixtures were investigated, at various gas velocity, jetsam concentration, particle-size ratio, particle-density ratio, and bed-aspect ratio combinations. Axial and radial segregation profiles were obtained from frozen bed sectioning. Low-velocities were used in order to minimize the possibility of segregation during bed collapse. In size-segregating systems, coarse particles act as jetsam, with a nearly constant concentration of fines in the flotsam-rich section. For density segregation, heavier particles act as jetsam and segregation behavior is not monotonically dependent on bed composition. A slight radial segregation was observed at all gas velocities, with jetsam accumulating near the wall. In size-and-density-segregating systems, denser particles (smaller and lighter) act as jetsam, with a slightly higher jetsam accumulation near the core of the bed. At higher gas velocities, however, the bottom layers become richer in jetsam in the periphery. Collectively, the data provide a robust experimental data set for evaluating the ability of existing and new models to predict species segregation. © 2007 American Institute of Chemical Engineers *AIChE J,* 53: 2804–2813, 2007
Keywords: species segregation, axial segregation, radial segregation, concentration profile, gas-fluidized, binary, experimental, Geldart B

Introduction

Since their introduction in chemical industries, fluidized beds have been researched extensively in an effort to improve the various processes that rely on them.[1–3] Due to the large number of industrial processes that depend on the fluidization of fine (e.g., catalytic cracking of petroleum) or coarse particles (e.g., coal combustors for electricity generation), a strong emphasis has been placed on understanding how differences in particle size determine the fluidization behavior of monodisperse systems, namely, that fine particles fluidize differently than coarse ones.[4] Less emphasis has been placed on bridging the gap between understanding single-species (monodisperse) behavior and predicting multiple-species (polydisperse) interactions important to pharmaceutical and chemical industries alike (as in drug manufacturing and production of high-grade alumina, Al_2O_3, or titania, TiO_2). A better understanding of the bed dynamics, including mixing and segregation of two or more species, is of particular relevance to the pharmaceutical industry,[5,6] where it is important to guarantee that small drug particles uniformly blended into a matrix of larger ingredients do not separate during fluidized-bed drying prior to tableting.

Segregation in fluidized beds has been extensively studied during the past several decades. Numerous segregation mechanisms (percolation, granular temperature gradients, bubbling, etc.) have been reported and the complex physics involved cannot be easily generalized. In systems where fine dusts are present, segregation has been linked to the bubbling

This article contains supplementary material available via the Internet at http://www.interscience.wiley.com/jpages/0001-1541/suppmat.

Correspondence concerning this article should be addressed to C. M. Hrenya at Hrenya@Colorado.edu.

patterns in the bed.[7] Rowe et al.[8] were the first to name the sinking component of a binary system *jetsam* and the rising component *flotsam*. They analyzed segregation by size difference, and concluded that the component separation is a consequence of bubble motion, as previously suggested by Zenz and Othmer.[7] Particles carried to the top of the bed by the wakes of bubbles percolate back down through the emulsion phase as a result of gravity, effectively sorting the solids into flotsam and jetsam.[9] For systems composed of different density particles, denser particles tend to act as jetsam, with a decreasing degree of segregation as velocity increases.[10] For systems composed of equal density particles, small particles tend to act as flotsam.[10–12] Segregation by size increases with increasing bed height, decreasing size of fines, increasing mean size, and as the gas velocity approaches the minimum fluidization velocity of the smaller particle.[13] For some conditions, however, a layer inversion has been observed,[14,15] wherein the species acting as flotsam and jetsam switch roles as the gas velocity increases.

Several competing factors contribute to the ultimate segregation state of a mixture of two or more species. To date, no first-principles model has been created that takes into account the complex interactions among gravity, drag force, gas-phase turbulence, and particle collisions, to mention a few factors. Van Wachem et al.[15] concluded that the dominant forces causing segregation are different depending on the gas velocity. At low-velocities the dominant force is the drag, whereas an increase in gas velocity brings about increasingly important effects of gradients in granular temperature and pressure. The work described herein is part of a bigger effort to determine, through a systematic experimental and numerical analysis of segregation, the relative abilities of existing models in predicting profiles of the flow field variables associated with fluidized mixtures. As a first step toward this goal, a binary Geldart group B experimental system is targeted in which the effects of drag force are expected to dominate. Such a system serves as a test bed that enables a critical comparison of existing drag laws for polydisperse systems.

Recent work by Leboreiro et al.[16] found, via simulation, that the form of the drag law has a significant impact on the qualitative nature of species segregation for (low-velocity) fluidized beds operating near the minimum fluidization. They tested four drag laws: the first, following Gidaspow,[17] is a combination of the Ergun[18] and the Wen and Yu[19] drag laws; the second follows the Benyahia et al.[20] implementation of the Hill, Koch, and Ladd[21,22] drag law, which was obtained from lattice-Boltzmann simulations. The third and fourth drag laws are modifications of the first two by a multiplicative factor, proposed recently by van der Hoef et al.[23,24] from lattice-Boltzmann simulations, that accounts for the binary nature of the system. The first two drag laws are the standard *ad hoc* modifications of monodisperse expressions, whereas the second two are derived specifically for polydisperse systems. The predictions obtained using the van der Hoef et al.[23] binary correction are markedly different than those of the *ad hoc* modification, thereby indicating the important influence the chosen drag law has on segregation in these systems.

Numerical models including these or other drag laws should be able to accurately predict a wide range of conditions. Comparisons to date between numerical predictions and experimental measurements have been restricted to the relatively limited set of experimental conditions available in the literature, and by the computational power available. The goal of this study to provide a diverse data set against which the predictions obtained from numerical models can be critically compared. Only a handful of researchers have reported combined experimental and computational investigations of segregation in bubbling gas-fluidized binary systems.[25–27] Huilin et al.[25] compared several size segregation profiles of binary Geldart group D mixtures with predictions, based on a multifluid gas-solid flow model where drag is derived from the Gidaspow[17] drag law, with good results. They caution about the importance of incorporating correct values for the collision parameters in simulations (in particular, for the restitution coefficient) in order to accurately capture the behavior of segregating systems. Bokkers et al.[26] compared the dynamic size segregation of Geldart group D particles—a single pseudo-2-D experimental set from the work by Goldschmidt et al.[12] described below—against numerical predictions based on the Gidaspow[17] drag law, with modest agreement. One study to date[27] has focused on the effect of drag laws on the prediction of segregation, comparing one data set from the work by Goldschmidt et al.[12] against simulations using various empirical and fundamental drag laws and concluding that using lattice-Boltzmann based drag laws[22,24] with the polydisperse correction proposed by van der Hoef et al.[23] attained the best prediction. While some of the numerical results described ealier indicate good agreement with the *ad hoc* treatment of polydisperse drag, others indicate good agreement with lattice-Boltzmann laws. Since the range of data used for experimental–numerical comparisons is extremely limited in all cases (in part due to the limited availability of a diverse data sets against which to compare), stating *a priori* which drag law holds the better prediction is difficult at best.

Several recent experimental contributions have focused on calculating a mixing index—a single *integrated* value that indicates the overall segregation state of a mixture—with relatively few studies reporting the segregation profiles needed to quantitatively evaluate the segregation predictions from numerical models. A survey of the experimental work to date on axial segregation[8,10–14,25,28–32] is presented in Table 1. The table indicates the various types of segregation targeted by each group of studies (size segregation, density segregation, or both size and density differences), the experimental conditions measured (steady-state or dynamic), as well as the geometry of the bed and the Geldart groups of the particles used. A list of the experimental parameters varied is also included, along with the measurement technique employed. Most of the work has focused on steady-state axial segregation measurements. The numerical work of Goldschmidt et al.[33] brings to attention that an accurate prediction of segregation dynamics is a key test for validation of fundamental hydrodynamic models. In the recent work by Leboreiro et al.[16] it is concluded that steady-state comparisons are also a tough test of the relative abilities of drag laws in predicting segregation. A summary of the axial segregation trends observed in the various experimental studies is also presented in Table 1. One additional contribution, by Wormsbecker et al.,[6] analyzed both radial and axial size segregation in a conical fluidized bed, based on a mixing index. Their axial

Table 1. Summary of Representative Prior Experimental Work on Segregation

Reference	Species Differentiation					Conditions		Geometry		Geldart Group			
	d_R	ρ_R	S:DL	S:DH	L:D	SS	dyn.	2D	3D	C	A	B	D
[A] Rowe et al.,[8] Rowe and Nienow,[10] Naimer et al.,[28] Nienow et al.[29]	✓	✓	—	✓	—	✓	—	✓	✓	—	✓	✓	✓
[B] Geldart et al.[13]	✓	✓	—	✓	—	✓	—	—	✓	—	—	✓	✓
[C] Wu and Baeyens[11]	✓	✓	—	✓	—	✓	—	—	✓	—	✓	✓	✓
[D] Rasul et al.,[14] Rasul and Rudolph[30]	—	✓	—	✓	—	✓	—	—	✓	✓	✓	✓	—
[E] Marzocchella et al.,[31] Olivieri et al.[32]	✓	✓	✓	✓	✓	✓	✓	—	✓	—	—	✓	—
[F] Goldschmidt et al.[12]	✓	✓	✓	✓	✓	✓	✓	✓	—	—	—	—	✓
[G] Huilin et al.[25]	✓	✓	—	✓	—	✓	—	—	✓	—	—	—	✓
[H] This study	✓	✓	—	✓	—	✓	—	—	✓	—	—	✓	—

Ref.	Parameters	Principal Measurements	Reported C.P.	Reported M.I.	Trends
[A]	u, x, d_R, H_R	Frozen bed sieving	few	✓	Size-difference systems easiest to mix; jetsam: large particles. Mixing↑ with presence of standpipe or perforated distributors. M.I. a logistic function of u.
[B]	u, d_R	Frozen bed sieving	few	few	Size segregation↑ when $d_{\text{fines}}\downarrow$, $d_{\text{mean}}\uparrow$, or $u \rightarrow u_{mf}$. Jetsam: large particles.
[C]	u, d_R	Frozen bed sieving	few	✓	Segregation↑ when $H_R\downarrow$ ($H_R < 0.8$) or visible bubble flow rate↓. Jetsam: large particles.
[D]	u, x, d_R	Visual observation of layers	—	—	Segregation↑ when visible bubble flow rate↓. Whatever component maximizes bulk density will act as jetsam.
[E]	u	Pressure time-trace analysis	few	✓	Concentration of fluidized top layer and defluidized bottom layer independent of initial mixture concentration.
[F]	u, x, H_R	Digital image analysis	—	✓*	Segregation↑ and segregation rate↑ when $H_R\downarrow$ or $x\uparrow$. Jetsam: large particles.
[G]	x, d_R	Frozen bed sieving	✓	✓	Segregation↑ as $u\downarrow$. Jetsam: large particles.
[H]	u, x, d_R, H_R	Frozen bed sieving	✓	—	(in this manuscript)

Segregation focus nomenclature: d_R — different size, same density; ρ_R — different density, same size; S:DL — small is denser and lighter; S:DH — small is denser and heavier; L:D — large is denser. Conditions: SS — steady-state segregation; dyn. — dynamic segregation. Reported results: C.P. — concentration profiles; M.I. — mixing indices. Parameters varied: u — gas velocity; x — jetsam concentration; d_R — particle size ratio; ρ_R — particle density ratio; H_R — bed aspect ratio.
*In lieu of a mixing index, Goldschmidt et al.[12] report a *percentage of segregation*, an integrated quantity based on the average height of the species.

results are consistent with the findings summarized in Table 1. Radially, they observed an accumulation of coarse particles near the center bottom at low-gas velocities, and hypothesized that this accumulation is a consequence of insufficient upward force to carry the coarse particles up in the dilute core region of the conical bed. Most experimental studies have focused on segregation in binary gas-fluidized systems, where each component is of different size and same density, or of different density but the same size. Less emphasis has been placed on system composed of two species which differ in density, as well as size, despite these systems being of particular interest to many industrial processes (like the production of high-grade alumina and titania, or in fluidized-bed combustion). The bulk of the work has been done on axial segregation, and the most commonly reported measure of segregation is the mixing index, with very few studies reporting the localized species concentration measurements in three-dimensions (axial, radial, and azimuthal profiles) that better enable validation of theoretical models. This work addresses the aforementioned shortcomings.

The objective of this study is to provide a robust experimental test bed for critically comparing the relative ability of models, existing and new alike, to predict species segregation. Localized axial, radial, and azimuthal segregation measurements are sought. Several factors are considered in defining the base system. At low-fluidization velocities the effect of drag is expected to be dominant on species segregation.[15] In addition, low-velocities minimize the possibility of segregation upon bed collapse ("freezing") since they present small bed expansions during operation, thereby eliminating the impact of segregation during the free fall of particles. Furthermore, segregation is expected at lower velocities and mixing is expected at higher velocities and the results from Leboreiro et al.[16] indicate that the distinction between drag models is most apparent in the low-velocity regime. Finally, in order to avoid potential differences in behavior between the low-velocity nonbubbling and bubbling regimes of Geldart group A powders, this experiments focus on Geldart group B particles, which always display a bubbling behavior. With these considerations in mind, the scope of this study is

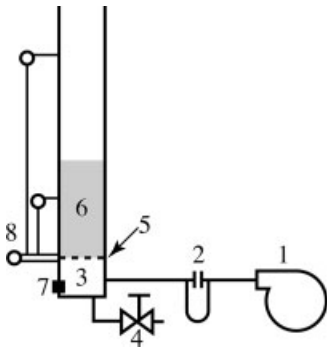

Figure 1. Experimental rig: (1) turboblower, (2) orifice flow meter, (3) plenum, (4) vent valve, (5) distributor plate, (6) particle bed, (7) plenum thermometer and hygrometer, and (8) differential pressure transmitters.

limited to low-velocity, gas-fluidized binary mixtures of Geldart group B particles. All relevant parameters (gas velocity, particle size and density, mass or volume fraction, and bed aspect ratio) are systematically varied, and the corresponding segregation profiles determined. Segregation profiles are reported since they preserve enough information to enable localized, detailed comparisons between experiments and numerical calculations, whereas mixing indices only reflect the overall state of the bed. In a follow-up article, numerical simulations using various drag laws are compared against the data set in this study in order to evaluate the current ability of drag laws to capture segregation over a wide range of conditions.

Experimental Setup and Methodology

This effort targets the segregation of two Geldart group B species fluidized by air at atmospheric pressures and temperatures. The effort is restricted to a low-velocity (no carryover of particles) bubbling bed (always bubbling since the materials are Geldart group B). The bed is fluidized in a Plexiglas column either 12 cm or 18.5 cm in dia., with the chosen diameter explicitly indicated for each experiment. The experimental rig is shown in Figure 1. A Mott Corporation 316 stainless steel porous plate with an average porosity of 10 μm and a 1.6 mm thickness acts as distributor plate. A Yaskawa V7 variable frequency drive controls a Fuji Electric VFD5 regenerative blower that provides the air for fluidization. The superficial velocity u, reported at local atmospheric conditions (1 kg/m^3 density and 1.83×10^{-5} Pa·s viscosity), is determined based on upstream measurements from a Lambda Square Oripac 4150-P orifice plate flow meter. The operating air temperature and relative humidity in the plenum are measured by means of an Omega HX93AV-RP1 humidity/temperature transmitter. The pressure drops across the orifice plate flow meter, across the distributor plate, from above the distributor plate to a point 20 cm above it, and across the entire fluidized bed are measured using Orange Research 20100 Series low-differential pressure transmitters with the ±0.2% accuracy option.

Species selection

Bubbles are usually associated with enhanced mixing in fluidized beds, and as such Geldart group B particles are of particular interest in the study of segregation, since bubbling is always present during their fluidization. The various particles examined are detailed in Table 2. The diameters d correspond to the cut between two consecutive standard sieve meshes. The density ρ was determined with a Quantachrome multipycnometer; the mass m of an average particle is also listed. Shape variations in monodisperse particles are usually quantified using a sphericity Φ, defined, as the ratio between the surface area of a sphere of the same volume as the particle, and the surface area of the particle itself $\Phi = S_{sph}/S_{part}$. For a sphere $\Phi = 1$; for nonspherical particles, $\Phi < 1$. Instead of a sphericity, Table 2 lists a calculated geometric factor ϕ. This geometric factor, provided as a convenience for comparing with the widely-used Gidaspow[17] drag law, is determined from experimental data as a fitting parameter to Ergun's equation for the measured pressure drop ΔP across the bed as a function of u in the packed-bed region, where the particle diameter is replaced by an apparent diameter $\phi(d_{\min}+d_{\max})/2$. Thus, in addition to accounting for shape variations, the fitting parameter ϕ captures the particles' polydispersity about the mean, and, hence, is not limited to values less than unity. While monodisperse species were targeted, a slight polydispersity is to be expected between the consecutive sieve cuts.

The various mixtures of glass and polystyrene used in this study are presented in Table 3, along with their corresponding mass loadings M, and the column dia. D used. The table lists the complete fluidization velocities u_{fc} of the mixtures investigated. It should be mentioned that for a binary mixture the concept of minimum fluidization velocity u_{mf} is not necessarily applicable, as illustrated in Figure 2 for the fluidization of a typical binary mix. Gauthier et al.[34] point out that there exists a transition domain in the $\Delta P - u$ diagram between the point where the first particles begin to fluidize, u_{fi}, and the point where all the particles are fluidized u_{fc}. This change in slope is most evident when fluidizing a layered system, where the species are initially placed one on top of the other, although in some cases it is also seen during slow defluidization of an initially well-mixed system. Tabulated values for $\Delta P - u$ for all mixtures are available online

Table 2. Properties of the Particles Used

Material	Legend	d (μm)	ρ (kg/m^3)	m (μg)	ϕ	ε_{max}	u_{mf} (cm/s)
Lead-free glass	G116	106–125	2476	1.99	0.966	0.564	1.8
	G231	212–250	2476	16.0	0.944	0.587	5.6
Polystyrene	P231	212–250	1064	6.87	0.981	0.572	2.9
	P275	250–300	1064	11.6	1.021	0.574	4.0
	P328	300–355	1064	19.7	0.994	0.575	5.4

Table 3. Characteristics of the Mixes Used

Materials (% mass)	D (cm)	M (kg)	u_{fc} (cm/s)	ε_{max}	H_{fc} (cm)
25/75 G116/G231	18.4	8.000	4.4	0.595	21.2
50/50 G116/G231	18.4	8.000	3.7	0.604	21.1
50/50 G116/G231	12.0	4.000	3.7	0.595	23.9
75/25 G116/G231	12.0	4.000	3.5	0.594	24.3
46/54 P231/P328	18.4	6.000	6.0	0.605	35.0
20/80 G231/P231	12.0	1.800	5.4	0.573	23.1
50/50 G231/P231	12.0	2.000	6.9	0.572	21.2
75/25 G231/P231	12.0	2.000	7.1	0.585	16.3
25/75 G116/P275	18.4	8.000	3.0	0.599	41.6
50/50 G116/P275	18.4	8.000	4.1	0.598	35.0
69/31 G116/P275	18.4	6.115	2.4	0.590	23.2
75/25 G116/P275	18.4	6.000	2.3	0.591	21.7

(Supplementary material: Fluidization data) in spreadsheet form. With the exception of the density difference systems, for most mixtures the change in slope within the transition region is barely noticeable, and roughly overlapping traces are followed during fluidization and defluidization. For the purposes of this study, u_{fc} was determined visually from each one of the experimental fluidization curves, and was defined as the velocity beyond which the pressure drop across the bed stabilizes at the pressure corresponding to the bed mass loading. The maximum packing fractions ε_{max} in Table 3 are determined from the average bed height of three to five fully mixed, settled beds at a certain loading. The bed heights H_{fc} at complete fluidization indicate the average bed height at the corresponding velocities u_{fc} for the given mass loading M.

Methodology

This study focuses primarily on relatively low-fluidization velocities, namely velocities just above u_{fc}. At these low-velocities, segregation is expected to be predominantly caused by particle drag and gravity, as suggested by van Wachem et al.,[15] with granular temperature and granular pressure playing a negligible role. Low-gas velocities afford the additional benefit of small bed expansions during operation, thereby minimizing the possibility of segregation during bed collapse ("freezing") like that described by Cooper and Coronella.[35] Species segregation measurements have been performed for several superficial velocities using the mixtures detailed in Table 3; the results are discussed in the following section. The steps followed on each experimental trial (mixing at high-velocity, fluidization at velocity of interest, freezing, bed sectioning, species separation, and weighing) are now described in detail.

In order to guarantee repeatable initial conditions, it was first necessary to determine an adequate mixing method. A trial run was performed with a bed composed of 4 kg of glass and 4 kg of polystyrene (50/50 G116/P275) at a superficial velocity of 12cm/s, well above u_{mf} for either material (about 3 u_{fc} for the mixture), for 30 min. The subsequent analysis confirmed a well-mixed composition. A 30-min mixing stage at a gas velocity in excess of 3 u_{fc} was used for all subsequent experiments. After the initial mixing period described earlier, the gas velocity was adjusted to a target value, and the system was held at this velocity for a stabilization time. Following the stabilization period for a given trial, the air supply was rapidly shut off and the plenum vented to "freeze" the bed. The frozen bed was subsequently sliced in bands 4 cm in height or smaller using the slicing tool shown in Figure 3. Each of the 16 slicer sections was vacuumed out of the column. For trials with particles of different sizes, the species were separated by sieving and then weighed to determine the components' mass fractions with a 1% precision. For mixtures with same size particles (differing only in density), mass fractions were calculated from the bulk densities of the dry vacuumed-out sections to within 5%; the species were then separated by sink-float gravity classification in a 20% sodium chloride aqueous solution.

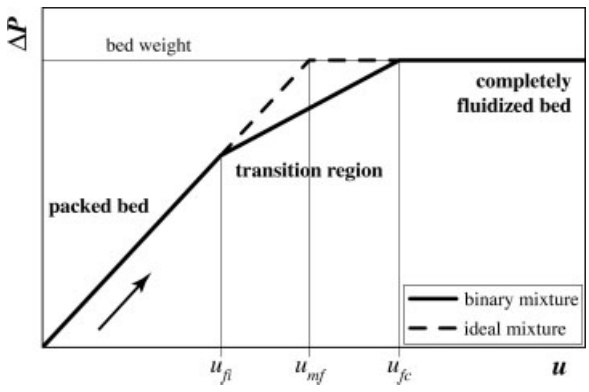

Figure 2. Representation of the differences between the fluidization curves for a typical binary mix and an ideal (nonsegregating) mixture on a ΔP-u diagram.

The minimum fluidization velocity u_{mf} is defined at the point at which the packed-bed slope intersects the bed weight pressure drop. A transition region is observed between the packed bed and completely fluidized regions, delimited by the incipient (u_{fl}) and complete (u_{fc}) fluidization velocities.

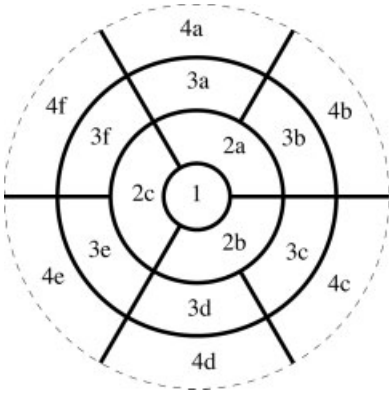

Figure 3. Top-view of the sectioning tool used.

Concentric sheetmetal circles 3.2, 8.3, and 13.3 cm in dia. are held together by sheetmetal plates, forming sections 1, 2a–c, and 3a–f; sections 4a–f are formed between the fluidized-bed walls and the sectioning tool.

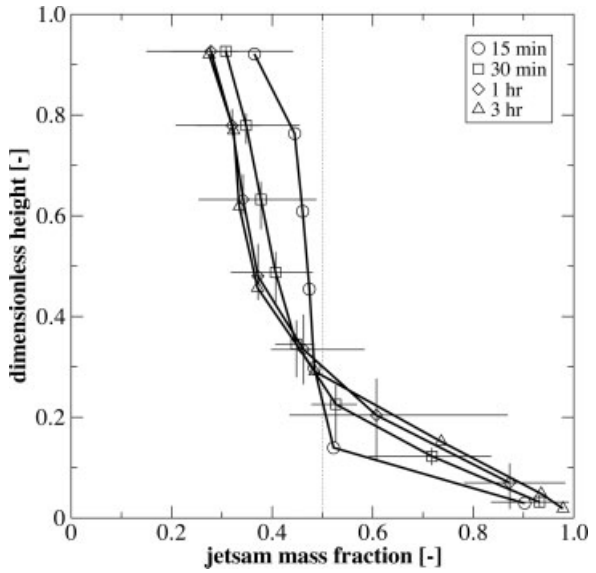

Figure 4. Segregation profiles for 8 kg 50/50 G116-P275 after 15 min, 30 min, 1 h, and 3 h stabilization times at u = 4.5 cm/s (1.1 u_{fc}); axes are fines' fraction vs. dimensionless bed height.

The components were fully mixed prior to each run.

Reproducibility

Care was taken to guarantee that the stabilization time was long enough to achieve a statistical steady state. Figure 4 shows the comparison among axial segregation profiles for the 50/50 G116/P275 mixture, obtained after stabilization times of 15 min, 30 min, 1 h, and 3 h. The 30-min and 1-h profiles are the averages of 5 and 3 experimental runs, respectively, with the error bars indicating the full ranges of the data; the 15-min and 3-h profiles correspond to single experimental runs. The spread in the dimensionless height data is a consequence of variations in slice thickness when vacuuming out the bands of the frozen bed. As the stabilization time increases, the profiles converge toward a final state. The figure shows that 1 h is a sufficiently long stabilization time for statistically repeatable measurements. This conclusion was further verified with the 50/50 G116/G231 mixture in the narrow column. Segregation profiles obtained after 1 h and 60 h were found to be overlapping, thereby ruling out the possibility that much longer stabilization times than 1 h were necessary. A 1-h stabilization time was chosen for all subsequent experiments.

Results and Discussion

In what follows, representative segregation curves are shown for the various mixtures explored, and their features are compared. The complete set of segregation experimental measurements is available online (Supplementary Material: Segregation Data) in spreadsheet form. As shown in Table 1, much has been published on mixing and segregation in binary gas-fluidized systems, where each component is of different size and same density (d_R), or of different density but same size (ρ_R), with a lesser emphasis on systems, where both are different. In this latter case, there are three possibilities: that the smaller particles are denser and heavier (S:DH) or denser and lighter (S:DL), or that the larger particles are denser (L:D). Only the second one of these possibilities is explored here since species in the S:DL size and density ranges have fairly similar minimum fluidization velocities, and, therefore, better provide a dataset for critically evaluating the ability of various drag laws to predict species segregation.

In order to keep the bed expansion to a minimum as to eliminate potential segregation during bed collapse, and given that as $u \rightarrow u_{mf}$ segregation increases,[13] the experiments were carried out at velocities close to u_{fc}. In order to verify that there is no significant segregation induced by the bed collapse, the "frozen" segregation measurements for a 50/50 G116/G231 mixture were compared with measurements performed vacuuming out the top layer of the bed while still fluidized. The jetsam concentration on the top layer of the running bed was found to be slightly higher than the corresponding one on the collapsed bed, but within the experimental uncertainty.

For the case of size segregation, the coarse particles act as jetsam, consistent with all previous findings in the literature (see Table 1). Measurements for three mixtures of glass (25/75 G116/G231, 50/50 G116/G231, and 75/25 G116/G231) are presented in Figure 5. Measurements were also performed for mixtures of polystyrene (46/54 P231/P328, figure not shown). For systems where the bed aspect ratio $H/D <$ 0.8, segregation by size is not significantly impacted by the bed height.[11] As shown in Table 3, H/D was kept at values greater than unity for all experimental runs. In order to verify that the results are not impacted by H/D, runs were done

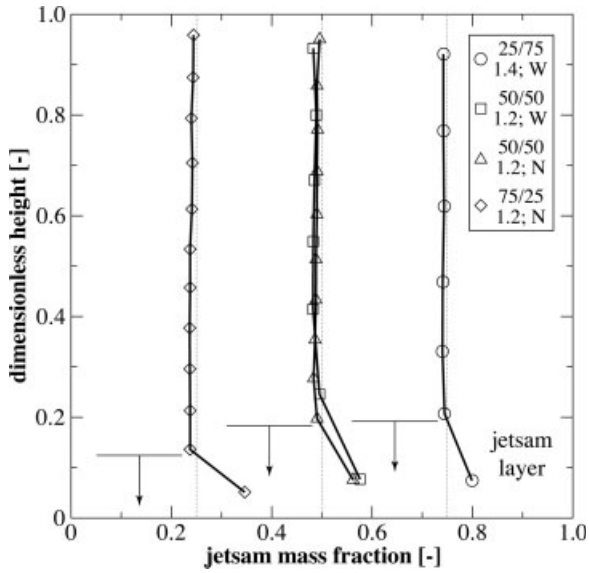

Figure 5. Effect of jetsam concentration on size segregation (d_R = 2).

Three glass mixtures (25/75 G116/G231, 50/50 G116/G231, and 75/25 G116/G231) are shown, fluidized at gas velocities between 1.2 u_{fc} and 1.4 u_{fc} in both the narrow (12.0 cm) and wide (18.4 cm) fluidization columns. The vertical dotted lines correspond to fully-mixed systems.

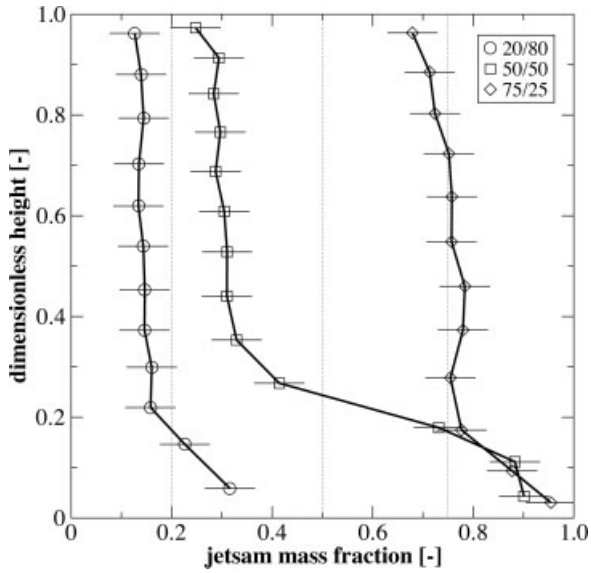

Figure 6. Effect of jetsam concentration on density segregation (ρ_R = 2.3) at low-gas velocity (about 1.1 u_{fc}).

Three glass-polystyrene mixtures (75/25 G231/P231, 50/50 G231/P231, and 20/80 G231/P231) are shown. The error bars correspond to the 5% uncertainty in the bulk-density-based concentration measurements (see the Methodology section). The vertical dotted lines correspond to fully-mixed systems.

with both the narrow and wide fluidization columns for the 50/50 G116/G231 mixture. It can be seen in Figure 5 that the results are overlapping for H/D = 1.15 and H/D = 2. Figure 5 also shows for all cases that the concentration of flotsam in the top layer of the segregated beds is only slightly larger than the corresponding concentration for a fully-mixed bed. In fact, very little size segregation was observed in any of the experiments, except for a small, jetsam-rich layer at the bottom of the bed. The dimensionless axial location of the interface separating the jetsam-rich layer from the rest of the bed—roughly corresponding to the point where the profiles cross the fully-mixed lines—increases slightly as the jetsam concentration increases, but is mostly independent of the initial mixture concentration, consistent with the observations of Marzocchella et al.[31]

For the case of density segregation, the denser particles act as jetsam. Measurements for three mixtures of glass and polystyrene (75/25 G231/P231, 50/50 G231/P231, and 20/80 G231/P231) are presented in Figure 6. Similar to what was seen in size-segregating systems, the density-segregating systems have a fairly constant concentration of flotsam in the layer above the jetsam-rich layer. Unlike the size-segregating systems, however, the shape of the concentration profiles is not maintained as the jetsam concentration increases, with the 50/50 G231/P231 system having the most segregated profile, and the systems rich in either species being better mixed (more vertical and closer to the fully-mixed line). The transition between flotsam and jetsam layers occurs below a dimensionless height of 0.3 for all cases, with the 50/50 G231/P231 system exhibiting the highest transition point. As mentioned previously, density segregation was determined from bulk density measurements of dry vacuumed-out sections of the bed, with a measurement uncertainty of approximately 5% indicated by the error bars in Figure 6. The fluidization curves of the density-segregating systems were the only ones where a transition region like that represented in Figure 2 was observed, suggesting that these systems segregate strongly at velocities between u_{mf} and u_{fc}.

Binary segregation profiles for S:DL systems were obtained for glass-polystyrene mixtures at various gas velocities (from $1.2u_{fc}$ up to $3.2u_{fc}$) and concentrations (25/75 G116/P275, 50/50 G116/P275, 69/31 G116/P275, and 75/25 G116/P275). The effect of fines' concentration on segregation is shown in Figure 7 for low-gas velocities ($1.2u_{fc}$), and in Figure 8 for high-gas velocities ($2.2u_{fc}$). In these systems the fines—the less massive although denser particles—act as jetsam. The shape of the concentration profiles is not maintained as the concentration of fines increases, with the system becoming better mixed for higher fines' concentrations. The trend is noticeable both at low- and high-velocities. For low-fines' concentrations (25/75 G116/P275), a clear layer of jetsam forms with the remainder of the bed having a fairly uniform composition. The addition of more fines both blurs the distinction between the jetsam and flotsam layers and causes the concentration to be more dependent on the axial position along the bed—the profiles further depart from the vertical. For high-velocities and high-concentrations of fines (right-hand side of Figure 8) the mixing becomes too violent for the relatively small amount of jetsam available to preferentially sink, leading to an almost uniformly mixed bed.

The effect of increasing gas velocity on segregation is further explored in Figure 9. The chosen mix (69/31 G116/P275) corresponds to a system with 50% glass and 50% polystyrene by volume. At low-velocity ($1.2u_{fc}$) the species are

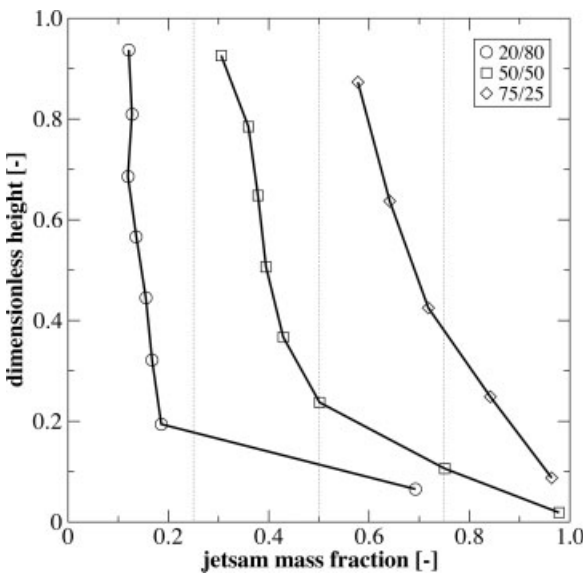

Figure 7. Effect of jetsam concentration on binary density and size (S:DL) segregation at low-velocity (about 1.2 u_{fc}).

Three glass-polystyrene mixtures (25/75 G116/P275, 50/50 G116/P275, and 75/25 G116/P275) are shown. The vertical dotted lines correspond to fully-mixed systems.

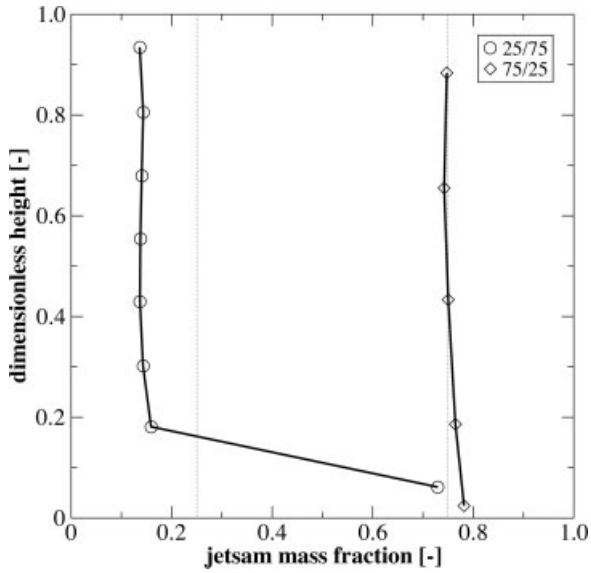

Figure 8. Effect of jetsam concentration on binary density and size (S:DL) segregation at high-velocity (about 2.2 u_{fc}).

Two glass-polystyrene mixtures (25/75 G116/P275 and 75/25 G116/P275) are shown. The vertical dotted lines correspond to fully-mixed systems.

distributed in an almost uniform gradient of decreasing concentration of fines with height. As the gas velocity is increased (1.6, 1.9, and 2.3u_{fc}), the amount of accumulated jetsam shrinks and the overall bed becomes better mixed, with the upper half of the concentration profiles becoming closer and closer to the fully-mixed vertical line. For a gas velocity of 3.2u_{fc} the system is almost perfectly mixed.

The possibility of radial and azimuthal segregation was also investigated by means of the slicing tool depicted in Figure 3. No azimuthal segregation patterns were identifiable in the experiments. Measurements from the 50/50 G116/P275 system (1 experimental set) seemed to indicate a slight jetsam accumulation toward one angular sector of the bed. This apparent segregation is a consequence of the frozen bed experimental technique. In the radial direction, the bed wall imposes a ring-like structure on the bubbling pattern and overall segregation. Due to the system's symmetry, these rings dynamically shift in the azimuthal direction. Depending on when the bed is frozen, these shifts are seen as slight azimuthal variations in species concentration. For verification purposes, a series of 20 experiments was run where the bed was fluidized and frozen every 20 to 30 s. Examination of the surfaces of the frozen beds confirmed the absence of an overall azimuthal pattern. Further exploration is required in this area, since the study of temporal variations in segregation is intractable with frozen bed experiments.

In the case of size-segregating systems (eight experimental sets), a relatively higher accumulation of jetsam is evident toward the periphery of the bed for all the studied compositions, with the bed becoming better mixed at higher gas velocities. The peripheral jetsam accumulation, which results in a concave plot of jetsam mass fraction as a function of radial position, is most evident at the bottommost layer of the bed. This result is inconsistent with the findings of Wormsbecker et al.[6] for a conical fluidized bed. In this cylindrical bed, the profiles observed can be linked to the bubble growth and circulation patterns in the bed. Small bubbles form at the surface of the distributor plate and coalesce into larger bubbles as they rise, moving toward the middle of the column since there are no bubbles with which to coalesce at the wall. As part of the circulation in the bed, particles travel downwardly near the wall. Due to the fast transition into a jetsam layer in size-segregating systems (Figure 5), the downwardly flow preferentially deposits jetsam near the periphery.

Radial segregation was also studied for the S:DL systems (15 experimental sets) and the segregation profile near the bottom of the bed was found to transition from concave to convex at gas velocities below 2u_{fc}. Two representative radial concentration profile sets are shown in Figure 10, one at 3.2u_{fc} and one at 1.6u_{fc}. Figure 10a, for higher gas velocities, shows that there is a relatively higher concentration of jetsam toward the center of the bed in the higher sections, with the opposite being true at the bottom, namely, a relatively higher concentration of jetsam toward the bed periphery. This result is consistent with the bed circulation pattern described earlier. As particles travel downwardly near the walls, flotsam from the top is carried toward the bottom, making the periphery flotsam-rich. At high-gas velocities, the jetsam depletion of the bottom center of the bed due to strong bubble transport causes a relatively higher concentration of jetsam to be present near the bottom periphery, as shown in Figure 10a. For lower gas velocities the relative accumulation of jetsam near the center of the column is observed throughout, as shown in Figure 10b. The less-vigorous bubbles in this latter

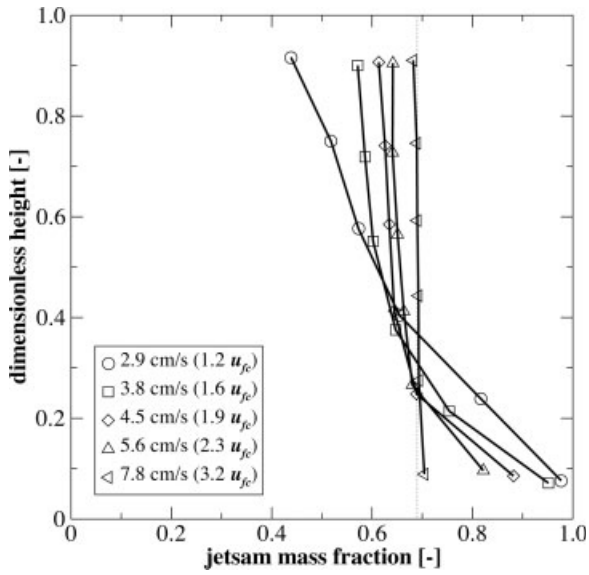

Figure 9. Effect of gas velocity on binary density and size (S:DL) segregation.

The mixture (69/31 G116/P275) represents an overall 50/50 concentration by volume. Measured gas velocities during operation are indicated in the legend. The vertical dotted line corresponds to a fully-mixed system.

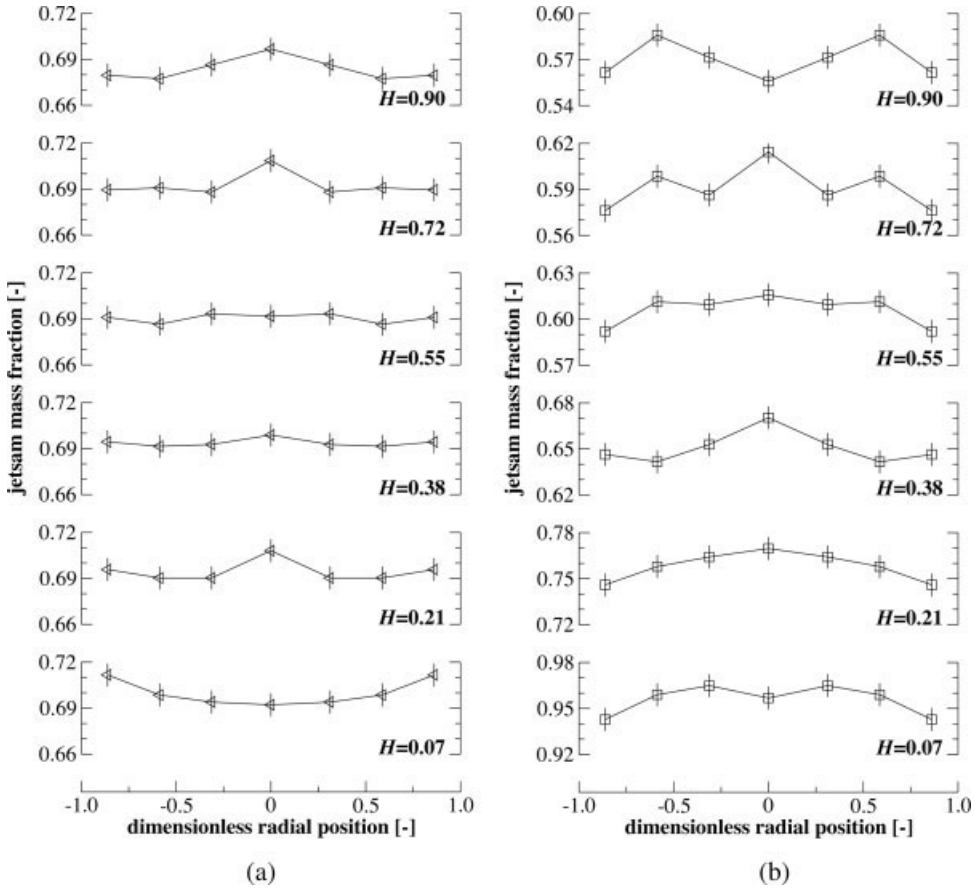

Figure 10. Radial segregation profiles at various heights for a binary density and size (S:DL, 69/31 G116/P275) system at (a) 3.2 u_{fc}, and (b) 1.6 u_{fc}.

The error bars correspond to the 1% uncertainty in the sieving-based concentration measurements. The symbols (◁, □) and dimensionless heights (H) correspond to those in Figure 9.

case preferentially carry flotsam up with them, leaving behind a relatively jetsam-rich center.

Concluding Remarks

Axial and radial segregation measurements of species segregation were done for binary Geldart group B mixtures of particles differing in size, density, or both. The measurements were obtained from frozen bed sectioning, with a particular emphasis in low-velocity systems (where drag is expected to be a dominant factor in segregation[15]) such that the possibility of segregation upon bed collapse was minimized. The results show a nonmonotonic behavior in density-segregating systems, whereby segregation is strongest for intermediate compositions, with fairly well mixed systems at low-or high-concentrations of jetsam.

Radial segregation was analyzed and the observed patterns were found to be dependent on fluidization velocity. For size-segregating systems a higher concentration of jetsam is found toward the bed periphery at all velocities, a consequence of the bed circulation pattern preferentially depositing jetsam near the wall and depleting it from the center due to bubble transport. For size-and-density-segregating systems, a higher concentration of jetsam is found toward the bed center when compared to the periphery at a given axial level. However, in high-velocity systems (where the components are axially well-mixed) a slight accumulation of jetsam is observed near the bottom periphery. For lower gas velocities, this tendency disappears and jetsam is seen to accumulate near the core of the bed. No azimuthal segregation patterns were observable, due to the temporal limitations of the frozen bed technique.

An extensive set of concentration profiles, suitable for critical evaluation of fluidization models, is available online as supplementary material in spreadsheet form. A follow-up article will compare these data set with numerical simulation predictions, based on the method described by Leboreiro et al.[16] in order to directly evaluate the relative abilities of *ad hoc* and lattice-Boltzmann-based polydisperse drag laws to capture segregation behavior in fluidized beds.

Acknowledgments

The authors wish to acknowledge the assistance provided by Dragan Mejic, Dana Hauschulz, and Matthew Lehr in the assembly and

instrumentation of the experimental system, and by Heather Woods and Thomas Walters in the development of the experimental technique. We are also thankful to Martin van der Hoef for providing preprints of two of his articles. This work is supported by the National Science Foundation Grant Opportunities for Academic Liaison with Industry (NSF GOALI) program under grant CTS-0318999, by the American Chemical Society Petroleum Research Fund under grant 43393-AC9, and by the University of Colorado Undergraduate Research Opportunities Program.

Literature Cited

1. Fan L-S. *Gas–Liquid–Solid Fluidization Engineering*. Boston: Butterworth-Heinemann; 1989.
2. Kunii D, Levenspiel O. *Fluidization Engineering*. 2 ed. Boston: Butterworth-Heinemann; 1991.
3. Yang W-C, ed. *Handbook of Fluidization and Fluid–Particle Systems*. New York: Marcel Dekker; 2003.
4. Geldart D. Types of Gas Fluidization. *Powder Technol*. 1973;7(5): 285–292.
5. Muzzio FJ, Shinbrot T, Glasser BJ. Powder technology in the pharmaceutical industry: the need to catch up fast. *Powder Technol*. 2002;124:1–7.
6. Wormsbecker M, Adams A, Pugsley T, Winters C. Segregation by size difference in a conical fluidized bed of pharmaceutical granulate. *Powder Technol*. 2005;153:72–80.
7. Zenz FA, Othmer DF. *Fluidization and Fluid–Particle Systems*. New York: Reinhold Publishing Corp.; 1960.
8. Rowe PN, Nienow AW, Agbim AJ. Preliminary quantitative study of particle segregation in gas-fluidized beds-binary systems of near-spherical particles. *Trans. Inst. Chem. Eng*. 1972;50:324–333.
9. Hoffmann AC, Janssen LPBM, Prins J. Particle segregation in fluidized binary-mixtures. *Chem Eng Sci*. 1993;48:1583–1592.
10. Rowe PN, Nienow AW. Particle mixing and segregation in gas-fluidized beds-review. *Powder Technol*. 1976;15:141–147.
11. Wu SY, Baeyens J. Segregation by size difference in gas fluidized beds. *Powder Technol*. 1998;98:139–150.
12. Goldschmidt MJV, Link JM, Mellema S, Kuipers JAM. Digital image analysis measurements of bed expansion and segregation dynamics in dense gas-fluidised beds. *Powder Technol*. 2003;138:135–159.
13. Geldart D, Baeyens J, Pope DJ, van de Wijer P. Segregation in beds of large particles at high velocities. *Powder Technol*. 1981;30(2): 195–205.
14. Rasul MG, Rudolph V, Carsky M. Segregation potential in binary gas fluidized beds. *Powder Technol*. 1999;103:175–181.
15. van Wachem BGM, Schouten JC, van den Bleek CM, Krishna R, Sinclair JL. CFD modeling of gas-fluidized beds with a bimodal particle mixture. *AIChE J*. 2001;47:1292–1302.
16. Leboreiro J, Joseph GG, Hrenya CM, Snider DM, Banerjee SS, Galvin JE. The influence of binary drag laws on simulations of species segregation in gas-fluidized beds. *Powder Technol*., in press.
17. Gidaspow D. *Multiphase Flow and Fluidization: Continuum and Kinetic Theory Descriptions*. London: Academic Press; 1994.
18. Ergun S. Fluid flow through packed columns. *Chem Eng Prog*. 1952;48(2):89–94.
19. Wen CY, Yu YH. Mechanics of fluidization. *Chem Eng Prog Symp Ser*. 1966;62(62):100–111.
20. Benyahia S, Syamlal M, O'Brien TJ. Extension of Hill–Koch–Ladd drag correlation over all ranges of Reynolds number and solids volume fraction. *Powder Technol*. 2006;162(2):166–174.
21. Hill RJ, Koch DL, Ladd AJC. The first effects of fluid inertia on flows in ordered and random arrays of spheres. *J Fluid Mech*. 2001;448:213–241.
22. Hill RJ, Koch DL, Ladd AJC. Moderate-Reynolds-number flows in ordered and random arrays of spheres. *J Fluid Mech*. 2001;448:243–278.
23. van der Hoef MA, Beetstra R, Kuipers JAM. Lattice-Boltzmann simulations of low-Reynolds-number flow past mono- and bidisperse arrays of spheres: results for the permeability and drag force. *J Fluid Mech*. 2005;528:233–254.
24. Beetstra R, van der Hoef MA, Kuipers JAM. Drag force of intermediate Reynolds number flow past mono- and bidisperse arrays of spheres. *AIChE J*. 2007;53(2):489–501.
25. Huilin L, Yurong H, Gidaspow D, Lidan Y, Yukun Q. Size segregation of binary mixture of solids in bubbling fluidized beds. *Powder Technol*. 2003;134:86–97.
26. Bokkers GA, Annaland MVS, Kuipers JAM. Mixing and segregation in a bidisperse gas–solid fluidised bed: a numerical and experimental study. *Powder Technol*. 2004;140:176–186.
27. Beetstra R, van der Hoef MA, Kuipers JAM. Numerical study of segregation using a new drag force correlation for polydisperse systems derived from lattice-Boltzmann simulations. *Chem Eng Sci*. 2007;62(1–2):246–255.
28. Naimer NS, Chiba T, Nienow AW. Parameter-estimation for a solids mixing segregation model for gas-fluidized beds. *Chem Eng Sci*. 1982;37:1047–1057.
29. Nienow AW, Naimer NS, Chiba T. Studies of segregation mixing in fluidized-beds of different size particles. *Chem Eng Commun*. 1987;62:53–66.
30. Rasul MG, Rudolph V. Fluidized bed combustion of Australian bagasse. *Fuel*. 2000;79:123–130.
31. Marzocchella A, Salatino P, Pastena VD, Lirer L. Transient fluidization and segregation of binary mixtures of particles. *AIChE J*. 2000;46:2175–2182.
32. Olivieri G, Marzocchella A, Salatino P. Segregation of fluidized binary mixtures of granular solids. *AIChE J*. 2004;50:3095–3106.
33. Goldschmidt MJV, Kuipers JAM, van Swaaij WPM. Hydrodynamic modelling of dense gas-fluidised beds using the kinetic theory of granular flow: effect of coefficient of restitution on bed dynamics. *Chem Eng Sci*. 2001;56(2):571–578.
34. Gauthier D, Zerguerras S, Flamant G. Influence of the particle size distribution of powders on the velocities of minimum and complete fluidization. *Chem Eng J*. 1999;74:181–196.
35. Cooper S, Coronella CJ. CFD simulations of particle mixing in a binary fluidized bed. *Powder Technol*. 2005;151:27–36.

Manuscript received Sep. 11, 2006, and revision received May 29, 2007, and final revision received July 17, 2007.